

Underwater Image Enhancement by the Retinex Inspired Contrast Enhancer STRESS

Michela Lecca^a

Fondazione Bruno Kessler, Digital Industry Center, via Sommarive 18, 38123 Trento, Italy

Keywords: Underwater Images, Image Enhancement, Retinex.

Abstract: Underwater images are often affected by undesired effects, like noise, color casts and poor detail visibility, hampering the understanding of the image content. This work proposes to improve the quality of such images by means of STRESS, a Retinex inspired contrast enhancer originally designed to process general, real-world pictures. STRESS, which is based on a local color spatial processing inspired to the human vision mechanism, is here tested and compared with other approaches on the public underwater image dataset UIEB. The experiments show that in general STRESS remarkably increases the quality of the input image, while preserving its local structure. The images enhanced by STRESS are released for free to enable visual inspection, further analysis and comparisons.

1 INTRODUCTION

Underwater imaging is an important support for navigation and for many activities of marine exploration, such as rescue missions, ecological monitoring, marine life studying, hand-made structure inspections (Manzanilla et al., 2019), (Bonin-Font et al., 2008), (Selby et al., 2011), (Lu et al., 2017), (Pedersen et al., 2019), (Matos et al., 2016), (McLellan, 2015), (Sheehan et al., 2020), (Ho et al., 2020), (Yin, 2021). For all these task, images with good visibility of details and content are required, but unfortunately underwater images are usually affected by low-light, non-uniform illumination, green-bluish color cast, haze and noise. These issues are mainly due to three physical phenomena of the transmission of the light through the water medium. First, in the water, the red component is absorbed faster than the green and the blue ones and this generates the green-bluish color that characterizes the underwater images. Second, there is the light background scattering, i.e. the diffusion of the light from sources others than the sample of interest, including also suspended particles that often generate noise. Third, there is the light forward scattering, i.e. the deviation of the light from its original angle of transmission, that attenuates the light energy aggravating the visibility of the details and content of the observed scene. Many image enhancement techniques have been developed and two recent, in-

teresting reviews are presented in (Li et al., 2019a), (Wang et al., 2019). In (Li et al., 2019a), these techniques are divided in two groups, named respectively the IFM-free image enhancement methods and the IFM-based image restoration methods, where 'IFM' stands for *image formation model*. The methods of the first class enhance underwater images without considering any physical model of the image formation in the marine environment. They usually process the input image by reworking its color distribution and contrast. Some examples of these methods are the works in (Hummel, 1977), (Zuiderveld, 1994), (Iqbal et al., 2010), (Huang et al., 2018), (Vasamsetti et al., 2017), (Jamadandi and Mudenagudi, 2019), (Fabbri et al., 2018). On the contrary, the methods of the second class rely on physical principles of the underwater imaging process. Basically, they assume that the image signal is determined by two energy components relative to the light directly transmitted from the observed scene to the camera and to the light background scattering. Some examples of these methods are the works in (Chao and Wang, 2010), (Serikawa and Lu, 2014), (Zhao et al., 2015), (Li et al., 2016a), (Li et al., 2016b), (Wang et al., 2017), (Shi et al., 2018) (Barbosa et al., 2018). Anyway, despite the many efforts on underwater image enhancement, this task is not yet solved and remains still today an active research field.

This work investigates the usage of the Retinex-inspired, real-world image enhancer STRESS (Kolås

^a  <https://orcid.org/0000-0001-7961-0212>

et al., 2011) as an IFM-free tool for improving the quality of underwater pictures. STRESS basically implements a local equalization of the red, green and blue channels. For each channel and for each pixel x , STRESS randomly samples a set of pixels around x and stretches the channel intensity distribution around x between two values selected from the sampled pixels. These values vary from pixel to pixel and form two surfaces bounding the channel and called *envelopes*. Stretching the channel between its envelopes increases the contrast granting a better visibility of the image details and content. The name STRESS is an acronym of the expression 'Spatio-temporal Retinex-like Envelope with Stochastic Sampling' which refers to the main characteristics of this algorithm and with the fact that it was originally applied for time sequence enhancement. Developed as a contrast enhancer for general, real-world image enhancer, STRESS is here tested as an IFM-free underwater image enhancer on the public, popular dataset UIEB (Li et al., 2019b), which contains 890 marine images with corresponding high quality references. The experiments show that STRESS remarkably improves the quality of the input image, increasing its contrast and dynamic range while preserving as much as possible its original structure. Moreover, compared with other algorithms of the same class, STRESS exhibits similar or better performance.

The paper is organized as follows: Section 2 describes STRESS; Section 3 explains how STRESS is evaluated in the framework of underwater image enhancement; Section 4 reports the results, while Section 5 draws some conclusions and future work.

2 STRESS

STRESS is a spatial color algorithm inspired by Retinex theory (Land et al., 1971), (Land, 1964).

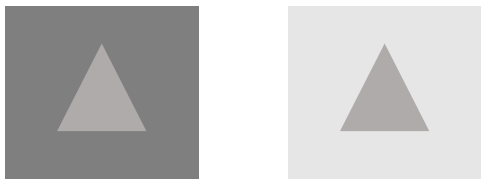


Figure 1: An example of simultaneous contrast: a same triangle is displayed against two different backgrounds, but the triangle seems to be brighter on left than on right. This is because the color of a point as perceived by humans is influenced by the surrounding colors.

Retinex was developed by Land and McCann at the end of 1970s as a model to predict how humans see colors. Based on a set of empirical evidences,

Retinex highlighted that human vision system and cameras work differently. In fact, when looking at a point of a scene, humans and cameras may report very different colors, as the simultaneous contrast phenomenon proves (see Figure 1). This is because the color of a point as perceived by the human vision system depends not only on the photometric properties of that point, but also on the surrounding colors. This fact suggested to Land and McCann to reproduce the human color sensation from a digital image by an algorithm, namely the Retinex algorithm, that reworks the colors of each pixel based on the spatial distribution of the colors of its neighbors. Local color processing is performed independently on the red, green and blue channels of the input image. This is in line with the empirical evidence that humans acquire and process separately the short, medium and long wavelengths of the light. The Retinex algorithm has been widely studied because its local spatial color analysis can be used to improve the visibility of image details and content as well as to attenuate or even remove possible color casts due to the light. Many variants of this processing mechanism have been developed and others are still under development, proposing different approaches to combine local spatial and color information with the final purpose to enhance the input image.

STRESS arises from the Milano Retinex family (Rizzi and Bonanomi, 2017), (Lecca, 2020), a set of algorithms grounded on Retinex principles and mainly used for image enhancement. These algorithms differ to each other in the definition of the spatial support where to compute the local spatial color distribution, in the way the spatial and channel intensity information are combined for improving the input image, and consequently in the final enhancement level. Precisely, STRESS is a variant of the Milano Retinex algorithm Random Spray Retinex (RSR) (Provenzi et al., 2007). RSR takes as input a color image and works separately on its color channels. For each channel I of the input image and for each pixel x of I with channel intensity $I(x)$, RSR computes N random sprays, i.e. N sets $S_1(x), \dots, S_N(x)$ of k pixels randomly selected with radial distribution around x . RSR extracts from each $S_i(x)$ the maximum intensity value M_i and maps the intensity $I(x)$ onto a new value $L(x)$, called the lightness of I at x and defined as:

$$L(x) = \frac{1}{N} \sum_{i=1}^N \frac{I(x)}{M_i} \quad (1)$$

where I is of course processed in order to prevent division by zero. The number k models the locality of the color processing, i.e. the higher k the higher the points sampled around x and closer to x . Considering more than one spray (i.e. $N > 1$) enables

to mitigate possible chromatic noise due to the random sampling. The final enhanced image is obtained by rescaling the values of each channel lightness over $\{0, \dots, 255\}$ and packing the rescaled lightnesses as a RGB image. Rescaling the value $I(x)$ by the maximum values over each sprays enables stretching the local distribution of the channel intensity, increasing the channel brightness and contrast, and, according to (Lecca, 2014), lowering eventual chromatic dominants of the light.

The algorithm STRESS originated from RSR to further improve the image contrast. As RSR, STRESS processes the channels of the input image separately and for each channel I it implements the pixel-wise random sampling scheme of RSR. Differently from RSR, STRESS extracts both the minimum and the maximum intensity of each spray sampled on I and uses these values to define two surfaces E_{low} and E_{up} , called envelopes and bounding the channel. The intensity values of the channels are then stretched pixel-wise between the corresponding values in the lower and upper envelopes. This operation locally stretches the local distribution of I , thus increases the contrast of the image improving the visibility of the image details.

Mathematically, given a pixel x of I and the N sprays $S_i(x) (i = 1, \dots, N)$, let $E_{low}^i(x)$ and $E_{up}^i(x)$ be the minimum and maximum intensities over the spray $S_i(x)$ and let $R_i(x)$ be their distance, i.e.:

$$E_{low}^i(x) = \min \{I(y) : y \in S_i(x)\}, \quad (2)$$

$$E_{up}^i(x) = \max \{I(y) : y \in S_i(x)\}, \quad (3)$$

$$R_i(x) = E_{up}^i(x) - E_{low}^i(x). \quad (4)$$

STRESS maps the value $I(x)$ onto a new value $v_i(x)$ basically obtained by stretching $I(x)$ between $E_{low}^i(x)$ and $E_{up}^i(x)$ when these are different, while set to 0.5 (i.e. in the middle of the possible intensity range) otherwise:

$$v_i(x) = \begin{cases} \frac{1}{2} & \text{if } R_i(x) = 0 \\ \frac{I(x) - E_{low}^i(x)}{R_i(x)} & \text{otherwise} \end{cases} \quad (5)$$

As in RSR, more sprays are considered to reduce undesired effects of the random sampling. Specifically, the values $R_i(x)$ and $v_i(x)$ are averaged over N :

$$R(x) = \frac{1}{N} \sum_{i=1}^N R_i(x), \quad v(x) = \frac{1}{N} \sum_{i=1}^N v_i(x). \quad (6)$$

The envelopes containing the channel I are computed as follows:

$$E_{low}(x) = I(x) - R(x)v(x), \quad (7)$$

$$E_{up}(x) = E_{low}(x) + R(x), \quad (8)$$

and the value of $I(x)$ is mapped on the value $STRESS(x)$ defined as:

$$STRESS(x) = \begin{cases} \frac{1}{2} & \text{if } E_{up}(x) = E_{low}(x) \\ \frac{I(x) - E_{low}(x)}{E_{up}(x) - E_{low}(x)} & \text{otherwise} \end{cases} \quad (9)$$

Figure 2 shows an image and its enhancement by STRESS, along with an example of random spray computed around the barycenter of the red channel pixels and the lower and upper envelopes of the red channel.

3 EVALUATION

The evaluation of the performance of STRESS employed as an IFM-free underwater image enhancer is carried out on the public dataset UIEB¹. This dataset contains 890 real-world images, some of them captured with the camera oriented from the seabed to the water surface, others acquired in the opposite direction. The UIEB scenes have been taken under different illuminations, including both natural and artificial lights as well as a combination of them. The images present different issues for enhancement, like e.g. low light, veil, noise, green-bluish color cast. For each image J , the dataset contains also the *reference* of J , i.e. a 'ground-truth' version of J having good quality. This reference has been selected by 50 volunteers from a set of versions of J enhanced by different algorithms. Some examples of images from UIEB are shown in Figure 3.

Assessing a quality of an image is a hard task, not yet fully agreed (Pedersen and Hardeberg, 2012) and in general a single measure does not suffice to capture all the features concurring to the image quality (Baricelli et al., 2020). Therefore, here the performance of STRESS has been evaluated by analyzing both no-reference and full-reference measures.

The no-reference measures considered here are:

1. the mean brightness of J (B): B is the mean value of the intensity of the mono-chromatic image BJ obtained by averaging pixel by pixel the three color channels of J ;
2. the mean multi-resolution contrast (C) (Rizzi et al., 2004): C is the mean value of pixel-wise contrasts c computed on multiple scaled versions of BJ ; in particular, the contrast $c(x)$ of a pixel x of any rescaled version of BJ is defined as the average of the absolute differences between the intensity at x and the intensities of the pixels located in a 3×3 window centered at x ;

¹https://li-chongyi.github.io/proj_benchmark.html

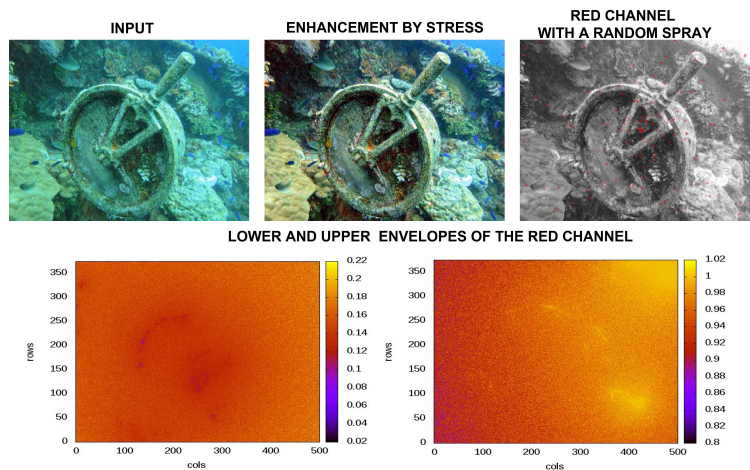


Figure 2: On top: an image, its enhancement by STRESS and its red channel, where the red circles belong to a random spray centered at the barycenter of the channel. On bottom: the lower and upper envelopes of the red channel computed using 10 sprays each with 250 pixels.

3. the histogram flatness (f): f measures the entropy of the intensity distribution of BJ and is defined as the L^1 distance between the probability density function of the intensity of BJ and the uniform probability density function;
4. the human vision system vision inspired metric UIQM (Panetta et al., 2015): this measure accounts for three features highly relevant to the human vision system to assess the readability of an underwater image, i.e. the colorfulness, the sharpness and the contrast of the image. UIQM has been designed to correlate with the human perception of the quality of an underwater image;
5. the underwater color image quality evaluation metric UCIQE (Yang and Sowmya, 2015): this measure, related to human perception, accounts for the chroma, the saturation and the contrast of the input image.

The values of B , C and f computed on the input image are compared with those computed on the output image. In general, an enhancer is expected to increase the brightness and the contrast, while decreasing the histogram flatness. The values of UIQM and UCIQE are expected to be proportional with the image quality, i.e. they should be high for images with good quality and low otherwise.

The full-reference metrics considered here are:

1. the mean square root (MSE): this is the L^2 distance between the reference image and the processed one and thus captures color distortions possibly introduced by enhancing;
2. the peak-signal-to-noise-ratio (PSNR): PSNR also measures differences between the reference

and the processed image but in a logarithmic space;

3. the structural similarity (SSIM) (Wang et al., 2004): this measure captures local distortions of the image structure accounting for the covariance of the image channel intensities in image sub-windows;
4. the percentage of enhanced images with red-distorted pixels (SP) and the percentage of red-distorted pixels in these images (MSP): in general, the red component of underwater images has low values and variance with respect to the other components. Stretching the variability range of the red channel in order to augment the information contained in may generate saturation. This means that the red values of some pixels are moved towards their maximum value, i.e. 255, introducing artifacts and making the image poorly natural. Such color distortions are here evaluated by detecting the pixels in the enhanced image such that (a) the red (R), green (G) and blue (B) components are close to red, i.e.:

$$R > 200 \ \& \ R > 10G \ \& \ R > 10B, \quad (10)$$

and (b) the inequalities in (10) do not hold for the corresponding pixels in the reference image. Mathematically, let p be a pixel in the enhanced image satisfying the inequalities of formula (10) and let p' be its corresponding pixel in the reference. If the color of p' does not match the conditions in (10), then p is considered as red-distorted. SP measures the percentage of enhanced images containing red-distorted pixels, while MSP is the percentage of red-distorted pixels in these images.

These measures compare the reference to the enhanced image. The lower the MSE, the higher the PSNR and the SSIM, the closer the enhanced image to the reference is. The higher the value of SP, the higher the quantity of red-distorted pixels is and the worse the quality of the enhanced image is. The higher MSP, the worse the enhancer performance on the test set is.

4 RESULTS

The images of UIEB have been processed by STRESS, where the number of sprays per pixel N is set to 10 and each spray contains $k = 250$ pixels. The images enhanced by STRESS are available for free by citing this paper² to enable visual inspection, further analysis and comparison. By the way, the performance of STRESS is compared with those obtained by six IFM-free underwater image enhancers, i.e.: the histogram equalization (HE) (Hummel, 1977), the contrast-limited adaptive histogram equalization (CLAHE) (Zuiderveld, 1994), the unsupervised von Kries based color correction via histogram stretching (UCM) (Iqbal et al., 2010), the global histogram stretching for underwater images working in the CIE Lab color space (RGHS) (Huang et al., 2018), the gamma correction algorithm (GC), the optimized version of RSR called Light-RSR (Banić and Lončarić, 2013) and the algorithm SuPeR (Lecca and Meselodi, 2019) from the Milano Retinex family. HE and CLAHE are popular algorithms processing the color histogram of the input image respectively globally and locally in order to maximize the image brightness and contrast. UCM corrects the image color and contrast by diminishing the blue intensity, increasing the red one, and reworking intensity and saturation on the HSI color space. RGHS increases the contrast by equalizing the green and blue components, redistributing the channel histograms and applying a bilateral filter to remove noise. GC increases the brightness and contrast of low light images by raising the channel components of the image by a factor γ , usually set to 2.2. Light-RSR is an optimized version of RSR, which uses a single spray per pixel ($N = 1$) and attenuates the chromatic noise by box filters. By this way, Light-RSR enhances the image similarly to RSR but with a much lower computation time. SuPeR is another, fast Milano Retinex algorithm, that improves the image by rescaling the channel intensities of any pixel x by a factor inversely proportional to the average of a set of intensities selected from tiles defined over the image and weighted by their distance from x .

²<https://drive.google.com/file/d/1XGjmhBaeuKucYSE3v6ekYPjkQgYIFEEX/view?usp=sharing>

All these algorithms have been run on UIEB by using their implementation available on the net. For Light-RSR, k is set to 250, for SuPeR the number of tiles per image is fixed to 25, while for the other algorithms the default parameters provided in their codes have been used. Figure 3 shows some examples of enhancement of UIEB images by these algorithms.

Table 1 reports the performance of STRESS in comparison with the other enhancers. The values of the different measures described in the previous Section are averaged on the number of images of UIEB and computed also for the original and reference images where this makes sense. On average, STRESS remarkably increases the image contrast, making it very close to that of the UIEB references, while the brightness remains close to that of the input images. STRESS also decreases the value of f making it close to that of the references, while returns the lowest (highest, resp.) value of MSE (PSNR, resp.) and a quite high value of SSIM, meaning that in the colors and the local structure of the enhanced images are close to those of the corresponding references. Moreover, STRESS returns quite high values of UIQM and UCIQE, close to those computed on the references. This indicates that STRESS provides in general natural images. Nevertheless, as already observed in (Li et al., 2019b), in some cases, the values of UIQM and UCIQE does not reproduce correctly the human perception about the naturalness of the underwater images. In fact, the algorithm HE often over-enhances the image, returning very bright pictures with many red-distorted pixels (see SP), but reports the highest values of UIQM and UCIQE, exceeding also those measured on the references. This unexpected behaviour is ascribed in (Li et al., 2019b) to the fact that the human perception in underwater environments is not yet fully studied and this adversely affects the modeling of metrics for the assessment of underwater images. A qualitative visual inspection of the results shows that HE and UCM are the worse algorithms in terms of red-distorted pixels and noise, while STRESS reports on average the 0.0158 % red-distorted pixels in the 5.73% of the images. The highest values of MSP are measured on images with very low-light regions or with very narrow red distribution (see for instance the last example in Figure 3).

On average, STRESS performs similarly to UCM and RGHS in terms of brightness, to CLAHE, RGHS and UCM in terms of contrast and flatness, to CLAHE and UCM in terms of UIQM, to RGHS and UCM in terms of UCIQE and to CLAHE and Light-RSR in terms of MSP. These observations, based on the quantitative analysis of the values in Table 1, are inline

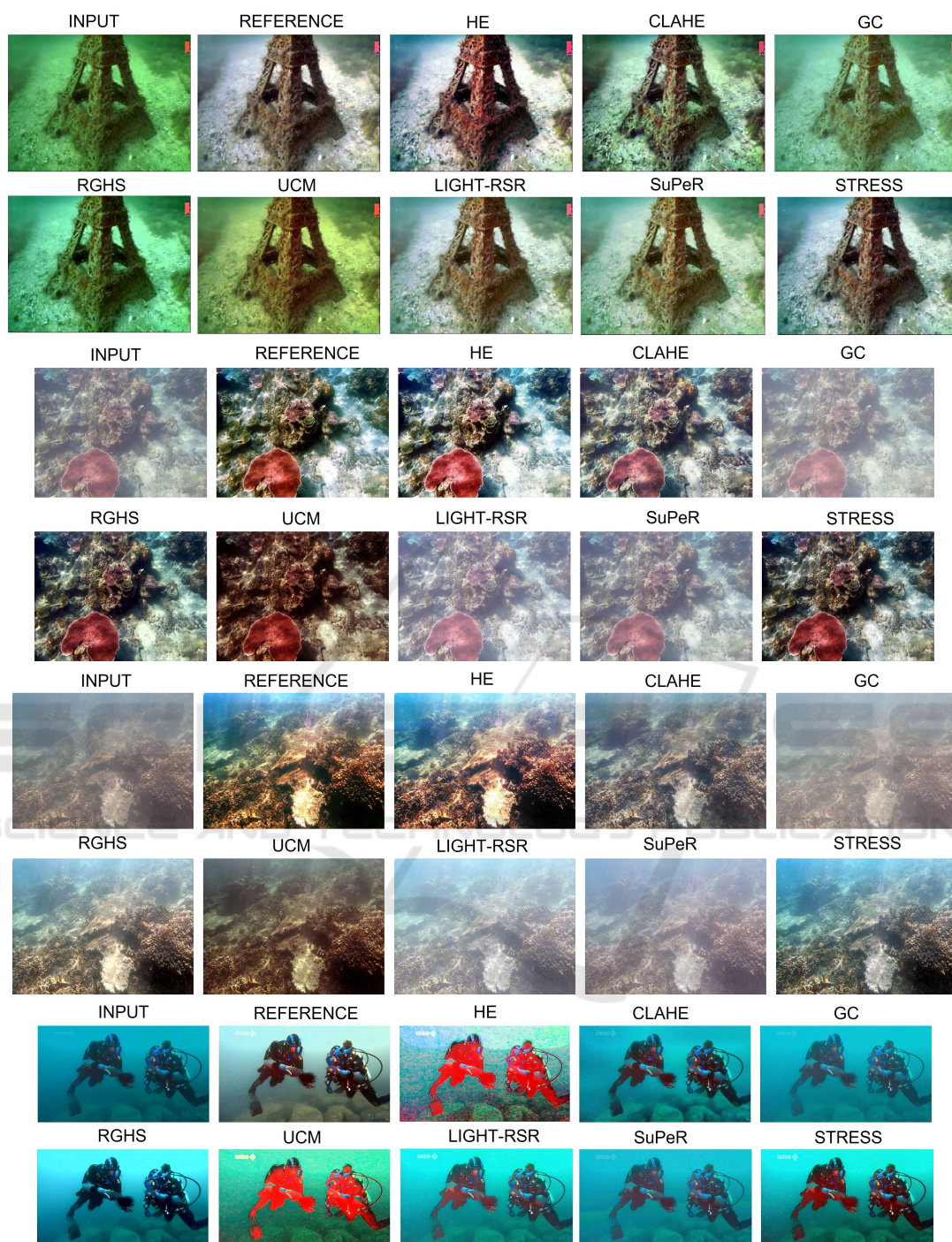


Figure 3: Examples of underwater image enhancement by different algorithms.

with the visual inspection of the images enhanced by these algorithms (see Figure 3 for an example).

5 CONCLUSIONS

This work presents the use of STRESS as underwater image enhancer, tests and compares it on the public data UIEB, making the results freely available to en-

Table 1: Image quality measures for different image enhancers applied on UIEB. INPUT and REFERENCE report respectively the values of B , C , f , UIQM and ICQE computed on the images and references of UIEB.

Algorithm	B	C	f [$\times 10^{-3}$]	MSE [$\times 10^3$]	PSNR	SSIM	UIQM	UCIQE	(SP, MSP)
REFERENCE	111.572	19.896	2.428	-	-	-	0.960	5.339	-
INPUT	106.405	11.869	3.936	1.768	17.355	0.773	0.542	4.189	-
HE	126.280	23.618	1.188	1.827	16.627	0.775	1.266	7.075	(28.764, 0.3535)
CLAHE	112.466	20.276	2.777	1.175	18.551	0.849	0.940	4.862	(1.124, 0.0122)
GC	136.915	11.756	3.982	2.423	15.519	0.753	0.702	3.687	(0, 0)
RGHS	104.232	17.476	2.617	1.152	19.222	0.825	0.768	5.775	(0.449, 0.0334)
UCM	104.406	18.366	2.708	1.662	17.464	0.799	0.934	6.044	(17.30, 0.3429)
LIGHT-RSR	132.524	14.869	3.321	1.997	17.339	0.808	0.816	4.596	(1.124, 0.0141)
SuPeR	133.517	13.678	3.565	2.159	16.804	0.783	0.797	4.219	(0.225, 0.0006)
STRESS	105.747	18.449	2.559	0.792	21.300	0.804	0.942	5.816	(5.730, 0.0158)

able visual inspection and further analysis and comparison. The experiments show that STRESS, originally devised as a real-world image enhancer and inspired by the local spatial color processing performed by the human vision system, effectively improves the contrast and the dynamic range of underwater images, preserving also their local structure and fidelity to references. The quality of the enhanced images is in general good and in line to or even better than other algorithms not based on underwater imaging physical models but used for this task. Nevertheless, the experiments also highlight one main issue that should be addressed in future work to guarantee better performance, i.e. the generation of red-distorted pixels that affect the quality of the enhanced images. Anyway, this problem is critical also for other algorithms, as shown by the results obtained by HE and UCM. In this respect, integrating in STRESS some physical information may help to overcome this problem, although this has been observed also for some IFM-based approaches, e.g. (Li et al., 2016b). In this framework, future work will theoretically and practically analyze and compare IFM-based methods against STRESS.

REFERENCES

- Banić, N. and Lončarić, S. (2013). Light random sprays retinex: exploiting the noisy illumination estimation. *IEEE Signal Processing Letters*, 20(12):1240–1243.
- Barbosa, W. V., Amaral, H. G., Rocha, T. L., and Nascimento, E. R. (2018). Visual-quality-driven learning for underwater vision enhancement. In *2018 25th IEEE Int. Conference on Image Processing (ICIP)*, Athens, Greece, pages 3933–3937. IEEE.
- Barricelli, B. R., Casiraghi, E., Lecca, M., Plutino, A., and Rizzi, A. (2020). A cockpit of multiple measures for assessing film restoration quality. *Pattern Recognition Letters*, 131:178–184.
- Bonin-Font, F., Ortiz, A., and Oliver, G. (2008). Visual navigation for mobile robots: A survey. *Journal of intelligent and robotic systems*, 53(3):263–296.
- Chao, L. and Wang, M. (2010). Removal of water scattering. In *2010 2nd int. conference on computer engineering and technology, Chengdu, China*, volume 2, pages V2–35. IEEE.
- Fabbri, C., Islam, M. J., and Sattar, J. (2018). Enhancing underwater imagery using generative adversarial networks. In *2018 IEEE Int. Conference on Robotics and Automation (ICRA)*, Brisbane, Australia, pages 7159–7165. IEEE.
- Ho, M., El-Borgi, S., Patil, D., and Song, G. (2020). Inspection and monitoring systems subsea pipelines: A review paper. *Structural Health Monitoring*, 19(2):606–645.
- Huang, D., Wang, Y., Song, W., Sequeira, J., and Mavromatis, S. (2018). Shallow-water image enhancement using relative global histogram stretching based on adaptive parameter acquisition. In *Int. conference on multimedia modeling, Bangkok, Turkey*, pages 453–465. Springer.
- Hummel, R. (1977). Image enhancement by histogram transformation. *Computer Graphics and Image Processing*, 6(2):184–195.
- Iqbal, K., Odetayo, M., James, A., Salam, R. A., and Talib, A. Z. H. (2010). Enhancing the low quality images using unsupervised colour correction method. In *2010 IEEE Int. Conference on Systems, Man and Cybernetics, Istanbul, Turkey*, pages 1703–1709. IEEE.
- Jamadandi, A. and Mudanagudi, U. (2019). Exemplar-based underwater image enhancement augmented by wavelet corrected transforms. In *Proc. of the IEEE/CVF Conference on Computer Vision and Pattern Recognition Workshops, Long Beach, CA, USA*, pages 11–17.
- Kolås, Ø., Farup, I., and Rizzi, A. (2011). Spatio-temporal Retinex-inspired envelope with stochastic sampling: A framework for spatial color algorithms. *Journal of Imaging Science and Technology*, 55(4):1–10.
- Land, E. (1964). The Retinex. *American Scientist*, 52(2):247–264.
- Land, E. H., John, and McCann, J. (1971). Lightness and Retinex theory. *Journal of the Optical Society of America*, 1:1–11.

- Lecca, M. (2014). *On the von Kries Model: Estimation, Dependence on Light and Device, and Applications*, pages 95–135. Springer Netherlands, Dordrecht.
- Lecca, M. (2020). Generalized equation for real-world image enhancement by Milano Retinex family. *J. Opt. Soc. Am. A*, 37(5):849–858.
- Lecca, M. and Messelodi, S. (2019). Super: Milano retinex implementation exploiting a regular image grid. *JOSA A*, 36(8):1423–1432.
- Li, C., Guo, C., Ren, W., Cong, R., Hou, J., Kwong, S., and Tao, D. (2019a). An underwater image enhancement benchmark dataset and beyond. *IEEE Transactions on Image Processing*, 29:4376–4389.
- Li, C., Guo, C., Ren, W., Cong, R., Hou, J., Kwong, S., and Tao, D. (2019b). An underwater image enhancement benchmark dataset and beyond. *IEEE Transactions on Image Processing*, 29:4376–4389.
- Li, C., Quo, J., Pang, Y., Chen, S., and Wang, J. (2016a). Single underwater image restoration by blue-green channels dehazing and red channel correction. In *IEEE Int. Conference on Acoustics, Speech and Signal Processing (ICASSP), Shanghai, China*, pages 1731–1735.
- Li, C.-Y., Guo, J.-C., Cong, R.-M., Pang, Y.-W., and Wang, B. (2016b). Underwater image enhancement by dehazing with minimum information loss and histogram distribution prior. *IEEE Transactions on Image Processing*, 25(12):5664–5677.
- Lu, H., Li, Y., and Serikawa, S. (2017). Computer vision for ocean observing. In *Artificial Intelligence and Computer Vision*, pages 1–16. Springer.
- Manzanilla, A., Reyes, S., Garcia, M., Mercado, D., and Lozano, R. (2019). Autonomous navigation for unmanned underwater vehicles: Real-time experiments using computer vision. *IEEE Robotics and Automation Letters*, 4(2):1351–1356.
- Matos, A., Martins, A., Dias, A., Ferreira, B., Almeida, J. M., Ferreira, H., Amaral, G., Figueiredo, A., Almeida, R., and Silva, F. (2016). Multiple robot operations for maritime search and rescue in eurathlon 2015 competition. In *OCEANS 2016-Shanghai*, pages 1–7. IEEE.
- McLellan, B. C. (2015). Sustainability assessment of deep ocean resources. *Procedia Environmental Sciences*, 28:502–508. The 5th Sustainable Future for Human Security (Sustain 2014).
- Panetta, K., Gao, C., and Agaian, S. (2015). Human-visual-system-inspired underwater image quality measures. *IEEE Journal of Oceanic Engineering*, 41(3):541–551.
- Pedersen, M., Bruslund Haurum, J., Gade, R., and Moeslund, T. B. (2019). Detection of marine animals in a new underwater dataset with varying visibility. In *Proc. of the IEEE/CVF Conf. on Computer Vision and Pattern Recognition Workshops, Long Beach, CA, USA*, pages 18–26.
- Pedersen, M. and Hardeberg, J. Y. (2012). Full-reference image quality metrics: Classification and evaluation. *Foundations and Trends in Computer Graphics and Vision*, 7(1):1–80.
- Provenzi, E., Fierro, M., Rizzi, A., De Carli, L., Gadia, D., and Marini, D. (2007). Random Spray Retinex: A new Retinex implementation to investigate the local properties of the model. *Trans. Img. Proc.*, 16(1):162–171.
- Rizzi, A., Algeri, T., Medeghini, G., and Marini, D. (2004). A proposal for contrast measure in digital images. In *Conference on colour in graphics, imaging, and vision, Aachen, Germany*, volume 2004, pages 187–192. Society for Imaging Science and Technology.
- Rizzi, A. and Bonanomi, C. (2017). Milano Retinex family. *Journal of Electronic Imaging*, 26(3):031207–031207.
- Selby, W., Corke, P., and Rus, D. (2011). Autonomous aerial navigation and tracking of marine animals. In *Proc. of the Australian Conference on Robotics and Automation (ACRA), Melbourne, Australia*.
- Serikawa, S. and Lu, H. (2014). Underwater image dehazing using joint trilateral filter. *Computers & Electrical Engineering*, 40(1):41–50.
- Sheehan, E. V., Bridger, D., Nancollas, S. J., and Pittman, S. J. (2020). Pelagicam: a novel underwater imaging system with computer vision for semi-automated monitoring of mobile marine fauna at offshore structures. *Environmental monitoring and assessment*, 192(1):1–13.
- Shi, X., Ueno, K., Oshikiri, T., Sun, Q., Sasaki, K., and Misawa, H. (2018). Enhanced water splitting under modal strong coupling conditions. *Nature nanotechnology*, 13(10):953–958.
- Vasamsetti, S., Mittal, N., Neelapu, B. C., and Sardana, H. K. (2017). Wavelet based perspective on variational enhancement technique for underwater imagery. *Ocean Engineering*, 141:88–100.
- Wang, N., Zheng, H., and Zheng, B. (2017). Underwater image restoration via maximum attenuation identification. *IEEE Access*, 5:18941–18952.
- Wang, Y., Song, W., Fortino, G., Qi, L.-Z., Zhang, W., and Liotta, A. (2019). An experimental-based review of image enhancement and image restoration methods for underwater imaging. *IEEE Access*, 7:140233–140251.
- Wang, Z., Bovik, A. C., Sheikh, H. R., and Simoncelli, E. P. (2004). Image quality assessment: from error visibility to structural similarity. *IEEE transactions on image processing*, 13(4):600–612.
- Yang, M. and Sowmya, A. (2015). An underwater color image quality evaluation metric. *IEEE Transactions on Image Processing*, 24(12):6062–6071.
- Yin, F. (2021). Inspection robot for submarine pipeline based on machine vision. *Journal of Physics: Conference Series*, 1952:022034.
- Zhao, X., Jin, T., and Qu, S. (2015). Deriving inherent optical properties from background color and underwater image enhancement. *Ocean Engineering*, 94:163–172.
- Zuiderveld, K. (1994). Contrast limited adaptive histogram equalization. *Graphics gems*, pages 474–485.